

Electronic Supporting information for: Supramolecular Squares of Porphyrazines

Kai Fan Cheng,^a Ngee Ai Thai,^a Lucile C. Teague,^b Klaus Grohmann,^a Charles Michael Drain^{*a,c}

Typical data for the characterization of the porphyrazine dimers and squares is presented below. Note that the various free base porphyrazines and the corresponding exocyclic coordinated adducts are somewhat labile to oxidation so are stored and manipulated under an inert atmosphere. The synthesis, properties, and potential applications of Pz are reported.¹⁻²⁵ The detailed characterization of the dimers is presented as a basis for the characterization of the the more complex squares, i.e. interpretation of the UV-Visible and NMR spectra. The MS of the dimers were consistent with the proposed structures.

Instrumentation.

MALDI-MS were done as a service by the facility at the University of Illinois at Urbana Champaign. ¹H NMR spectra were recorded on JEOL 400 MHz, a Varian VXR-300 MHz, or a Varian 500 MHz instrument. Chemical shifts are reported in ppm relative

to TMS. NMR assignments are consistent with those published previously. Agilent Technologies HP 1100 LC/MSD, and a Cary Bio-3 were used. Typical Electrospray Ionization Mass Spectroscopy (ESI-MS) method: ~0.05mM solutions in toluene were injected using acetonitrile/water (50:50 v:v) containing 1% trifluoroacetic acid, positive ion mode, and the fragmentor voltage between 100 and 350 V. AFM data were taken in tapping mode with a Park Scientific Instruments Auto Probe CP microscope under ambient conditions. Molecules were deposited on the freshly cleaved mica surface via drop-dry method, subsequently rinsed with toluene and dried under a stream of N₂.

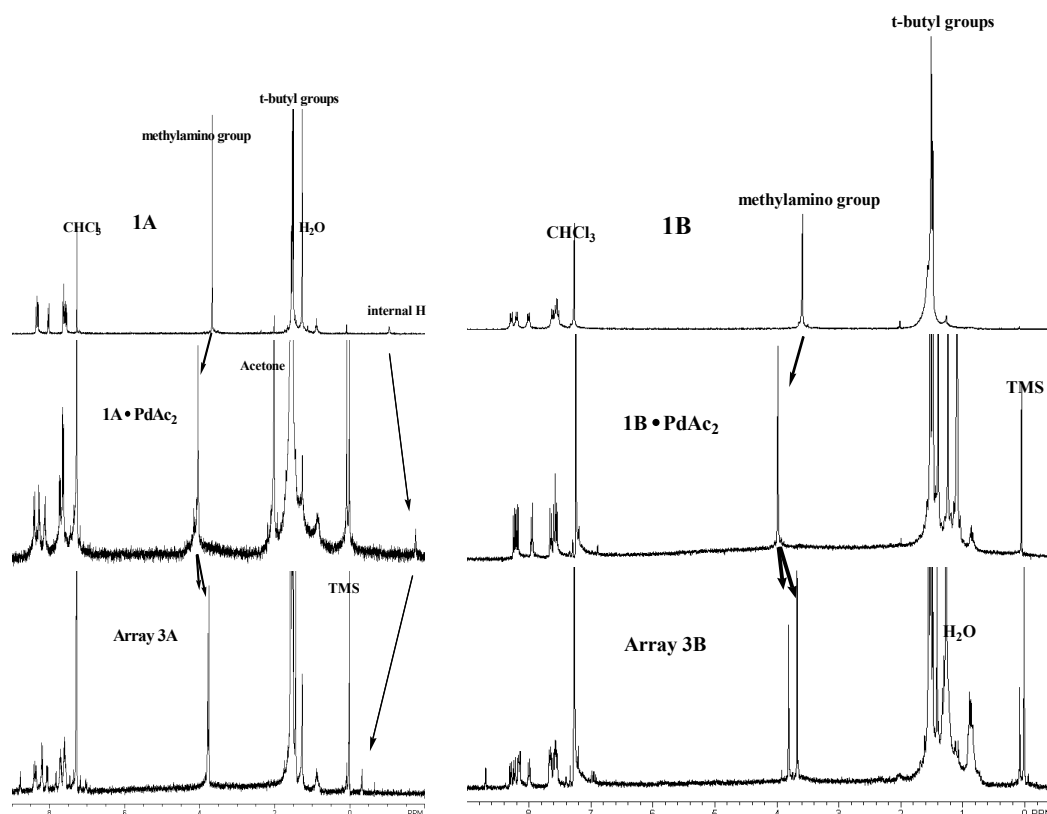


Figure ESI-1A. ¹H NMR (300 MHz) spectra of free base 2,3-bis(dimethylamino)-7,8,12,13,17,18-hexakis(4-(*tert*-butyl)phenyl)porphyrazine (top), its palladium adduct (middle), and dimer **Pd-3A** (bottom). Arrows indicate the chemical shift changes of the methylamino groups and internal pyrrole NH. **Figure SI-1B** ¹H NMR (300 MHz) of the dimer using the Ni(II) Pz gives a clearer indication of the chemical shift changes upon formation of the dimer. Spectra of 2,3-bis(dimethylamino)-7,8,12,13,17,18-hexakis(4-(*tert*-butyl)phenyl)porphyrazinato Ni(II), **1B**, (top), its palladium adduct (middle), and dimer **Pd-3B** (bottom). Arrows indicate the chemical shift changes of methylamino groups.

* cdrain@hunter.cuny.edu

Synthesis. The modifications of the Linstead¹ magnesium alkoxide templated macrocyclization reaction developed by Barrett and Hoffman²⁵ uses bis substituted maleonitriles, is quite versatile, and is the basis for the synthesis of the Pz building blocks herein. The use of two maleonitriles derivatives results in a statistical mixture of six Pz weighted by a variety of factors including stoichiometry, reactivity and solubility; nonetheless these compounds and isomers are readily separated and purified by flash chromatography. This strategy, in this case using 3,4-bis(4-*tert*-butylphenyl)pyrroline-2,5-diimine and bis(dimethylamino)-maleonitrile,³ is employed because all six of the products can be used as tectons or reference compounds and is easy to scale up. All Pz and the Ni(II) complexes (**1A**, **1B**, **2A**, **2B**, **5A**, **5B**) have ¹H

NMR, UV-visible, and mass spectra consistent with the structure and previous reports^{3,25} (see below). Since the Pd(II) assemblies are less stable than the corresponding Pt(II) arrays the yields in table 1 are spectroscopic for the former and isolated for the latter. The purification of adduct **5A-PtCl₂**, and arrays **6A** and **6B** is accomplished using flash chromatography (silica gel purchased from Seletco Scientific, 32-63 μm average particle size) using 1% methanol in dichloromethane as eluents. The R_f on TLC plate (Silica Gel 60 with a 254 nm fluorescent indicator) for **5A-PtCl₂**, **6A**, and **6B** are 0.8, 0.4 and 0.5, respectively using the same eluents.

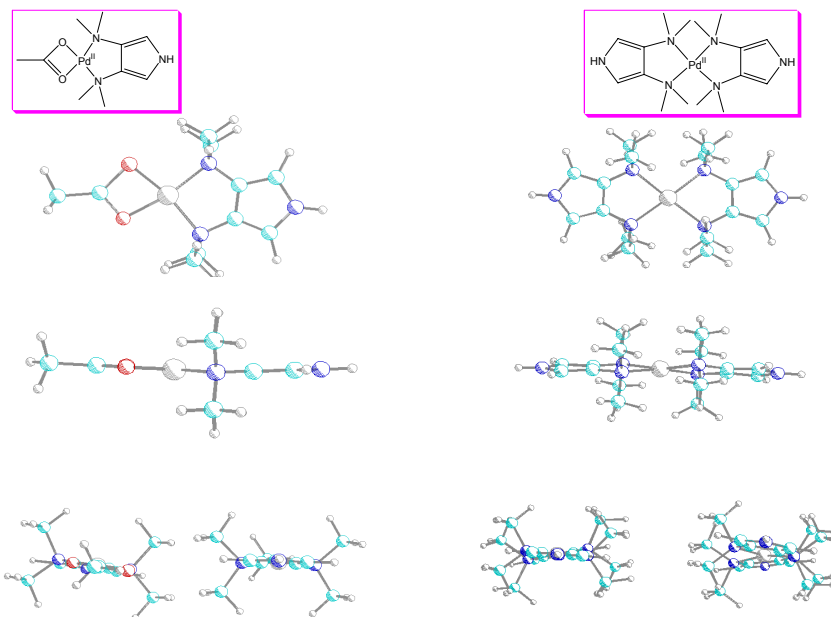


Figure ESI-2. Simple steric calculation using PC Model on the ligand binding sites of the monomer and dimer (for simplification the chromophores were replaced by the pyrrole rings) show the inequivalence of the methyl peaks in the Pt(II) dimers.

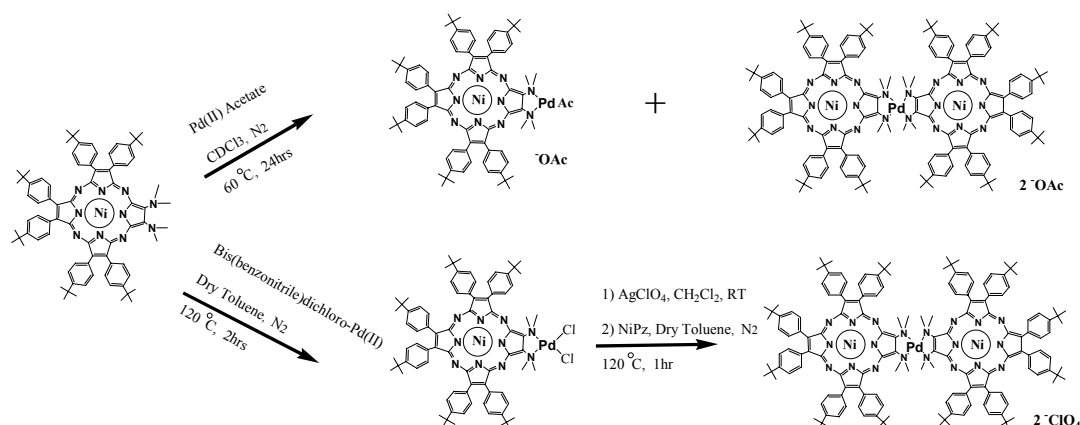


Figure ESI-3. Formation of the Ni(II) porphyrazine palladium adduct **1B-PdAc₂** and dimer **Pd-3B** via two different methods. ¹H NMR, MS and UV-visible spectra indicate the products are the same compounds. The Pt(II) adducts can be formed similarly. The bottom method is precedence for the formation of the squares by a similar route.

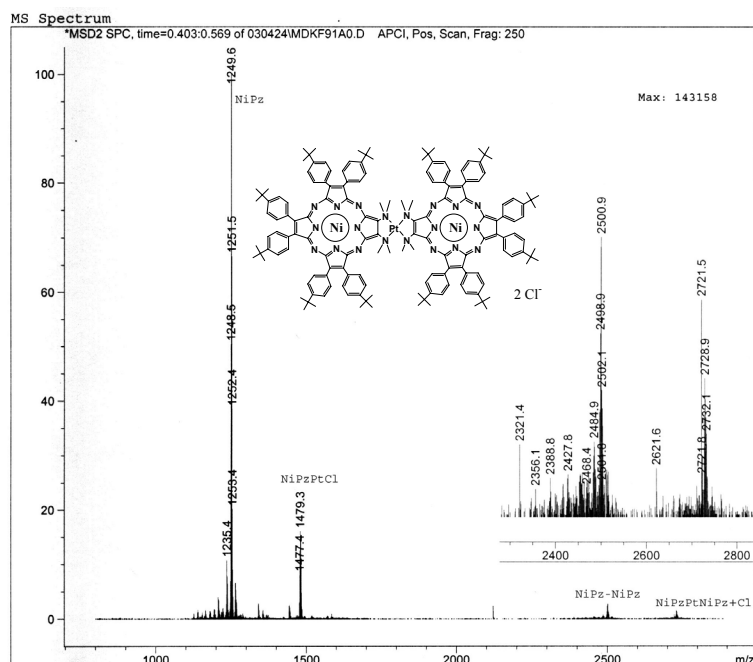


Figure ESI-4. Typical electrospray ionization mass spectra, in this case of the **Pt-3B** in positive-ion mode. 2729 (**Pt-3B** – Cl⁻). NiPz **1B** = 1249; **1B**•PtCl⁺ = 1479; **3B**•PtCl₂⁺ = 2764.

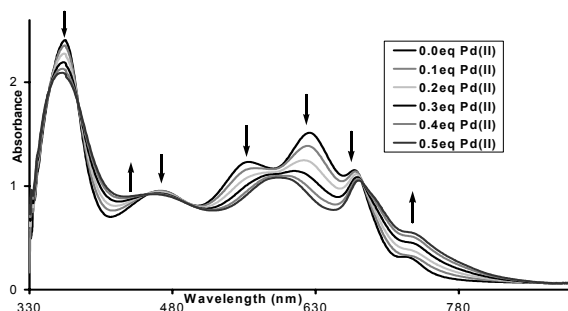


Figure ESI-5. Typical investigation of the self assembly processes. Formation of the dimer **Pd-4A** investigated by titration experiments, wherein aliquots of a Pd(OAc)₂ solution were added to the porphyrazine solution (50 μM in toluene), the mixture was stirred at room temperature for ~10min, and spectra were recorded at ~20 °C. The isosbestic points are an indication of the formation of one product. Only with a >4-fold excess of Pd(OAc)₂ does the dimer disassemble and the 1:1 adduct form.



Comparison of monomers and dimers using N(CH₃)₂ and NH₂ ligands on Pz

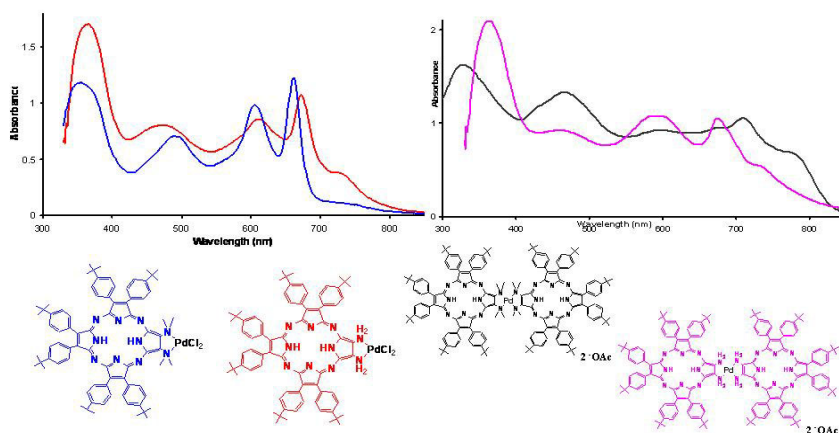


Figure ESI-6. Comparison of the UV-visible spectra in toluene (20 μM) of the Pd adducts of the Pz monomers with geminal dimethylamino and geminal amino ligands (left), and the Pz dimers (right). Colors of the structures correspond to the lines in the spectra.

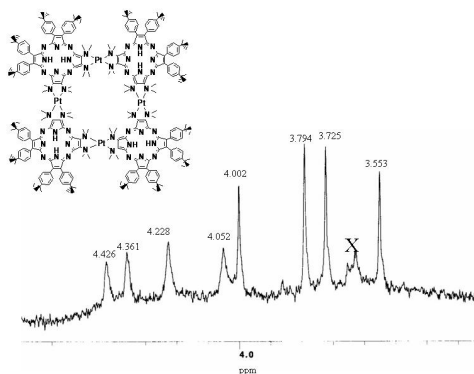


Figure ESI-7. $^1\text{H-NMR}$ of tetrameric square **6A** in the N-methyl group region indicates a substantial asymmetric twisting in the supramolecular square and that the inner methyl groups are differentiated from the outer methyl groups.

The $^1\text{H NMR}$ of the dimers show two resonances for the methyl groups due to a twisting about the metal, thus with the squares one expects the inner and outer methyl groups to be distinguishable and which would result in four peaks. With an asymmetric supramolecular conformation, eight peaks are expected – one for each methyl about the metal ion linker – which is observed (Figure ESI-7).

The UV-visible spectra of the monomers and adducts are qualitatively explained by the Gouterman 4-orbital model,^{26,27} and the observed changes upon formation of the dimers and square

arrays are explained in terms of Kasha's rules for transition dipoles²⁸ as applied to porphyrins.^{29,30} This latter model predicts splitting of the Soret band and to a lesser extent the Q bands because of the coupling of the two orthogonal excitons of each chromophore. Edge-to-edge coupling should be manifested as a red shift in the electronic spectra compared to the monomers, the corresponding adducts, and the dimers, as is observed. Since the square arrangement means that each Pz is electronically coupled to two other Pz at right angles, Kasha's model predicts that the absorptions band should broaden or split, which is also observed. Note that the Pt(II) and Pd(II) adducts are blue shifted relative to the free Pz because of the changes in the electron coupling of the nitrogen lone pairs to the π system, thus comparison of the adducts to the squares and dimers is appropriate.

UV-Vis peak maxima 20 μM in toluene nm (rel. abs): **5A**: 356 (1.503), 450 (0.477), 486 (0.530), 606 (0.581), 672 (0.538), 721 (0.433); **5A-Pt(II)**: 343 (0.869), 480 (0.456), 532 (0.487), 583 (0.662), 664 (0.431), 736 (0.249); Square **6A**: 340 (1.503), 528 (0.647), 586 (0.789), 662 (0.522), 695 (0.452). **5B**: 344 (1.57), 436 (1.03), 462 (1.14), 588 (1.22), 635 (1.11), 718 (0.84); **5B-Pt(II)**: 346 (1.60), 425 (0.90), 458 (1.00), 597 (1.07), 630 (1.13), 685 (0.97); **6B**: 345 (1.49), 459 (0.84), 492 (0.86), 622 (1.13), 690 (0.76), 738 (0.59). (Figure ESI-11)

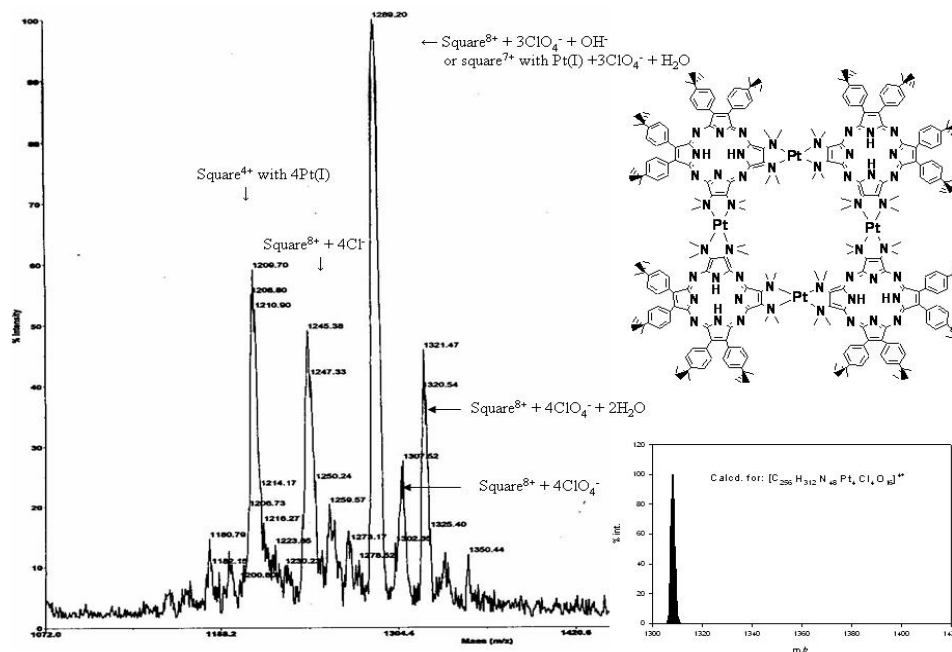


Figure ESI-8. MALDI-MS of tetrameric square **6A** from a chloroform solution is consistent with the structure. The water may be indicative of adducts or of oxidative reactions during the mass spectrometric analysis, and the reduction of the Pt(II) during MALDI analysis was also observed occasionally with the dimers. The Cl⁻ likely comes from traces of HCl in the CHCl₃. Inset: the low resolution calculated spectrum is for **6A** with four ClO₄⁻ counter ions.

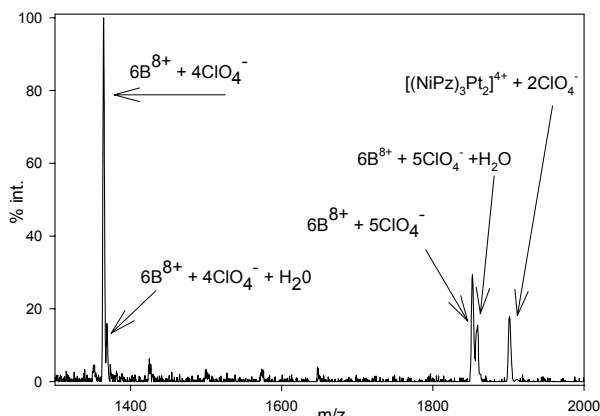


Figure ESI-9. MALDI-MS of tetrameric square **6B** from a chloroform solution is consistent with the structure. The water may be indicative of adducts or of oxidative reactions during the mass spectrometric analysis. The $[(NiPz)_3Pt_2]^{4+}(ClO_4)_2$ may be from decomposition in the MS or this compound may disassemble over time as this sample was about 6 months old when the MS was taken.

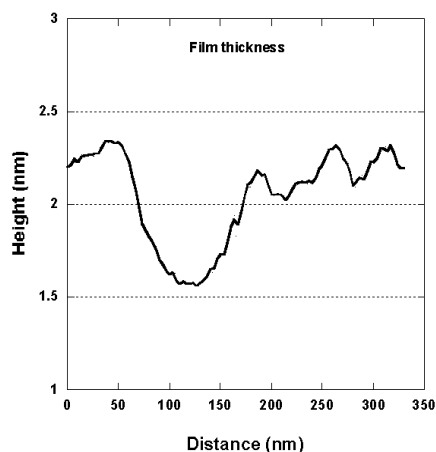


Figure ESI-10. A line trace from a nanoshaving experiment on a film of array **6A** on mica (see figure 2) indicates an average thickness of 0.5 nm; the expected width of the π systems of the Pz..

The preliminary AFM studies show that drop casting **6A** onto mica results in a monolayer film that corresponds to the supramolecular Pz array laying flat on the surface. (See the line trace from the nanoshaving experiment SI-10.) Control experiments using only Pz **5A** or **5A-PtCl₂** result in amorphous films of varied thicknesses. UV-Visible spectra of **6A** on mica are fundamentally similar to the solution phase spectra but with well understood and documented red shifts due to surface-molecule interactions and the “orientation” of the supermolecules. UV-Visible spectra of square **6A** on mica is essentially simmlary to that in solution but with modest red-shifts arising from surface deposition – a well documented effect. This indicates the arrays is in tact on this surface.

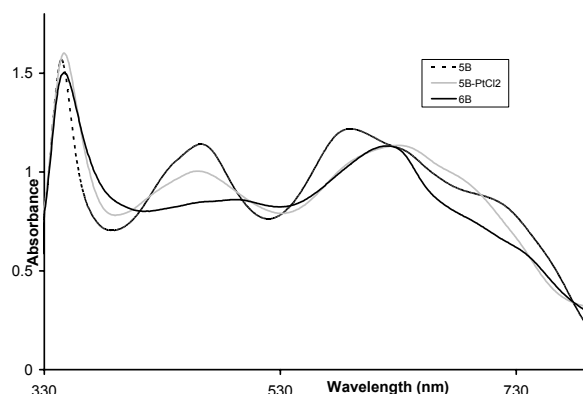


Figure ESI-11. UV-Visible of 5B, 5B-PtCl₂ and square array **6B**, 20 μ M in toluene.

Notes and references

- [1] A. H. Cook, R. P. Linstead, *J. Chem. Soc.* 1937, 929-932.
- [2] I. Salabert, T.-H. Tran-Thi, H. Ali, J. van-Lier, D. Houde, E. Keszei, *Chem. Phys. Lett.* 1994, **223**, 313-317. Optical and photophysical properties of self-assembled porphyrins and porphyrazines. First evidence of formation of mixed pentamers
- [3] T. F. Baumann, A. G. M. Barrett, B. M. Hoffman, *Inorg. Chem.* 1997, **36**, 5661-5665. Porphyrazine binaries: Synthesis, characterization, and spectroscopy of a metal-linked trinuclear porphyrazine dimer
- [4] A. G. Montalban, S. J. Lange, L. S. Beall, N. S. Mani, D. J. Williams, A. J. P. White, A. G. M. Barrett, B. M. Hoffman, *J. Org. Chem* 1997, **62**, 9284-9289. Seco-porphyrazines: Synthetic, structural, and spectroscopic investigations
- [5] T.-H. Tran-Thi, *Coord. Chem. Rev.* 1997, **160**, 53-91. Assemblies of phthalocyanines with porphyrins and porphyrazines: ground and excited state optical properties
- [6] D. P. Goldberg, A. G. Montalban, A. J. P. White, D. J. Williams, A. G. M. Barrett, B. M. Hoffman, *Inorg. Chem.* 1998, **37**, 2873-2879. Metal ion binding to octakis(dimethylamino)porphyrazine: Core coordination of Mn(III) and peripheral coordination of Pd(II)
- [7] D. P. Goldberg, S. L. J. Michel, A. J. P. White, D. J. Williams, A. G. M. Barrett, B. M. Hoffman, *Inorg. Chem.* 1998, **37**, 2100-2101. Molybdocene porphyrazines: A peripheral dithiolene metallacycle fused to a porphyrinic core
- [8] S. J. Lange, H. L. Nie, C. L. Stern, A. G. M. Barrett, B. M. Hoffman, *Inorg. Chem.* 1998, **37**, 6435-6443. Peripheral palladium(II) and platinum(II) complexes of bis(dimethylamino)porphyrazine
- [9] A. G. Montalban, H. G. Meunier, R. B. Ostler, A. G. M. Barrett, B. M. Hoffman, G. Rumbles, *J. Phys. Chem. A* 1999, **103**, 4352-4358. Photoperoxidation of a diamino zinc porphyrazine to the seco-zinc porphyrazine: Suicide or murder?
- [10] M. E. Anderson, A. G. M. Barrett, B. M. Hoffman, *J. Inorg. Biochem.* 2000, **80**, 257-260. Binding of octa-plus porphyrazines to DNA
- [11] L. A. Ehrlich, P. J. Skrdla, W. K. Jarrell, J. W. Sibert, N. R. Armstrong, S. S. Saavedra, A. G. M. Barrett, B. M. Hoffman, *Inorg. Chem.* 2000, **39**, 3963-3969. Preparation of polyetherol-appended sulfur porphyrazines and investigations of peripheral metal ion binding in polar solvents
- [12] A. G. Montalban, W. Jarrell, E. Riguete, Q. J. McCubbin, M. E. Anderson, A. J. P. White, D. J. Williams, A. G. M. Barrett, B. M. Hoffman, *J. Org. Chem* 2000, **65**, 2472-2478. Bis(dimethylamino)porphyrazines: Synthetic, structural, and spectroscopic investigations
- [13] E. G. Sakellariou, A. G. Montalban, H. G. Meunier, R. B. Ostler, G. Rumbles, A. G. M. Barrett, B. M. Hoffman, *J. Photochem. Photobio. A: Chemistry* 2000, **136**, 185-187. Synthesis and photophysical properties of peripherally metallated bis(dimethylamino)porphyrazines

- [14] A. A. Trabanco, A. G. Montalban, G. Rumbles, A. G. M. Barrett, B. M. Hoffman, *Synlett* 2000, 1010-1012. A seco-porphyrazine: Superb sensitizer for singlet oxygen generation and endoperoxide synthesis
- [15] S. L. J. Michel, B. M. Hoffman, S. M. Baum, A. G. M. Barrett, *Progress in Inorganic Chemistry*, 2001, **50**, 473-590. Peripherally functionalized porphyrazines: Novel metallomacrocycles with broad, untapped potential
- [16] E. G. Sakellariou, A. G. Montalban, H. G. Meunier, G. Rumbles, D. Phillips, R. B. Ostler, K. Suhling, A. G. M. Barrett, B. M. Hoffman, *Inorg. Chem.* 2002, **41**, 2182-2187. Peripherally metalated secoporphyrazines: A new generation of photoactive pigments
- [17] S. M. Baum, A. A. Trabanco, A. G. Montalban, A. S. Micallef, C. Zhong, H. G. Meunier, K. Suhling, D. Phillips, A. J. P. White, D. J. Williams, A. G. M. Barrett, B. M. Hoffman, *J. Org. Chem.* 2003, **68**, 1665-1670. Synthesis and reactions of aminoporphyrazines with annulated five- and seven-membered rings
- [18] M. Kandaz, S. L. J. Michel, B. M. Hoffman, *J. Porph. Phthal.* 2003, **7**, 700-712. Functional solitare- and trans-hybrids, the synthesis, characterization, electrochemistry and reactivity of porphyrazine/phthalocyanine hybrids bearing nitro and amino functionality
- [19] S. L. J. Michel, A. G. M. Barrett, B. M. Hoffman, *Inorg. Chem.* 2003, **42**, 814-820. Peripheral metal-ion binding to tris(thia-oxo crown) porphyrazines
- [20] A. G. Montalban, S. M. Baum, A. G. M. Barrett, B. M. Hoffman, *Dalton Trans.* 2003, 2093-2102. Studies on seco-porphyrazines: a case study on serendipity
- [21] E. G. Sakellariou, A. G. Montalban, S. L. Beall, D. Henderson, H. G. Meunier, D. Phillips, K. Suhling, A. G. M. Barrett, B. M. Hoffman, *Tetrahedron* 2003, **59**, 9083-9090. Novel peripherally functionalized seco-porphyrazines: synthesis, characterization and spectroscopic evaluation
- [22] M. Zhao, C. Stern, A. G. M. Barrett, B. M. Hoffman, *Angew. Chem. Int. Ed.* 2003, **42**, 462-464. Porphyrazines as molecular scaffolds: Periphery-core spin coupling between metal ions of a Schiff base porphyrazine
- [23] N. D. Hammer, B. J. Vesper, S. Lee, B. M. Hoffman, J. A. Radosevich, *Journal of Investigative Medicine* 2004, **52**, S350-S350. Structural correlation of the porphyrazines to biological activity
- [24] M. Zhao, C. Zhong, C. Stern, A. G. M. Barrett, B. M. Hoffman, *Inorg. Chem.* 2004, **43**, 3377-3385. Synthesis and properties of dimetallic M-1 Pz -M-2 Schiff base complexes
- [25] J. W. Sibert, T. F. Baumann, D. J. Williams, A. J. P. White, A. G. M. Barrett, B. M. Hoffman, *J. Am. Chem. Soc.* 1996, **118**, 10487-10493.
- [26] M. Gouterman, *The Porphyrins, Vol. 3*, Academic Press, New York, 1978.
- [27] M. Gouterman, G. H. Wagniere, L. C. Snyder, *J. Mol. Spectrosc.* 1963, **11**, 108-127. Spectra of porphyrins: Part II. Four orbital model
- [28] M. Kasha, H. R. Rawls, M. A. El-Bayoum, *Pure Appl. Chem.* 1965, **11**, 371.
- [29] C. A. Hunter, J. K. M. Sanders, *J. Am. Chem. Soc.* 1990, **112**, 5525-5534. The nature of pi-pi interactions
- [30] C. A. Hunter, J. K. M. Sanders, A. J. Stone, *Chem. Phys.* 1989, **133**, 395-404. Exciton Coupling in Porphyrin Dimers